

On the Placement and Sustainability of Drone FSO Backhaul Relays

Salim Janji, *Graduate Student Member, IEEE*, Adam Samorzewski, *Graduate Student Member, IEEE*,
Małgorzata Wasilewska, *Graduate Student Member, IEEE*, and Adrian Kliks, *Senior Member, IEEE*

Abstract—We consider free-space optical (FSO) communication links for the backhaul connectivity of small cells (SCs) where a UAV with an FSO apparatus can serve as a backhaul relay node. We demonstrate how such drone relay stations (DRSs) can be deployed in a high-rise urban area in order to provide FSO line-of-sight (LOS) links that are unobstructed by buildings. Also, in our solution we consider the case where solar panels are mounted on DRSs such that placing the DRS in a sunny location is prioritized, and we show the gain in terms of number of required trips to recharge the UAV.

I. INTRODUCTION AND RELATED WORK

Emerging cellular networks increasingly make use of small cells (SCs) as part of the strategy of densifying and shrinking cells in order to fulfill the high data rate and low latency requirements [1]. Furthermore, moving small cells such as those mounted on UAVs have received increased research as summarized by the surveys in [2] and [3]. Drone base stations (DBSs) can adapt their locations according to the changes in users' locations such that path loss and interference are reduced, and they prove to be a cost-effective replacement to fixed small cells structures. However, SCs require a robust backhaul connectivity during their operations [4], and providing backhaul connectivity to moving SCs is a technical challenge. In that context, free-space optical (FSO) communication links are found to provide superior performance relatively to radio frequency (RF) links because they achieve higher data rates, smaller antenna sizes leading to lower weight and volume, and increased security [5]. Deploying FSO transceivers on UAVs has received attention in recent years. The authors in [6] present a statistical channel model for FSO communication between a static transceiver and another one mounted on an UAV. In [7], the authors analyzed air-to-air (A2A) FSO communications using multirotors and showed that commercial multirotor drones can sustain an A2A FSO link despite the alignment difficulties according to the model they introduced. The authors in [8] consider a set of DBSs

with FSO transceivers whereas an FSO backhaul is provided to each DBS through FSO A2A links. They show that utilizing FSO for both backhaul and fronthaul substantially improves the system throughput. In [9], the authors were able to derive an approximation for the ergodic rate of an FSO link between an UAV serving as a relay and a ground station. Then, by combining it with an approximation for the ergodic sum rate of users served by the UAV through RF they obtained the ergodic rate of the relay. Similarly, UAVs serve as buffer-enabled FSO relays between stationary nodes in [10] enhancing the outage probability. However, the problem of placing antennas in locations such that a line-of-sight (LOS) link can be formed with the next hop without getting blocked by an obstacle is not considered since antennas are assumed to exist at a sufficiently large altitude whereas in this work, we consider that the obstacles are high enough to obstruct paths (e.g., high-rise urban area with skyscrapers). DRSs can also be placed at low altitudes in cases where they also establish RF links with ground nodes to limit interference to other nodes [11].

Moreover, UAVs flight duration is bounded by the on-board battery lifetime. To improve the energy performance, solutions can optimize for energy efficiency such as in [12] where the authors derived a model for the propulsion energy consumption taking the trajectory into consideration, and then they utilized it to optimize the trajectory of a UAV communicating with a ground terminal such that the energy efficiency is maximized. Alternatively, to cope with the limited on-board energy that DBSs have, the authors in [13] demonstrated a UAV prototype with solar panels. Also, the authors in [14] study the use of renewable energy sources by UAVs and formulate a signal-to-noise ratio (SNR) outage minimization problem which optimizes the transmit power and flight time of the UAV. Similarly in [15], the authors formulate a joint trajectory and resource allocation optimization problem in which a UAV can increase its altitude in the presence of clouds in order to harvest more energy. An algorithm is proposed to determine the UAV's trajectory in each time slot which takes into consideration the aerodynamic power consumption, on-board energy, and users' quality of service (QoS) requirements. However, in this work we consider the presence of high buildings that can obstruct both the light from the sun and the FSO link, and therefore the placement of DRSs should avoid both types of obstructions.

In this paper, we consider the problem of placing solar-powered DRSs to ensure backhaul connectivity to a given point between obstacles. First, we propose the use of Lee's visibility graph algorithm [16] to find the locations of DRSs such that

the LOS visibility is ensured between successive hops, and then we modify the algorithm so that placing DRSs in sunny locations is more preferable than in shadowed spots. We show that for the given environment the algorithm is able to place DRSs in sunny spots during all daytime hours. Furthermore, by adopting the energy models mentioned in literature, we show the gain in performance when using solar panels in terms of required number of recharge trips needed per day to sustain backhaul connectivity to a given destination.

The rest of the paper is organized as follows. Section II describes the considered scenario along with the power consumption model and energy harvesting and storage systems. Section III presents the solution for finding DRSs locations after constructing the visibility graph. In Section IV we extend the mechanism such that we also find sunny locations and prioritize choosing them in the shortest path algorithm. Furthermore, Section V presents the simulations results, and Section VI concludes the paper.

II. SYSTEM MODEL

A. Environment Description

We consider a high-rise urban area with a macrocell base station (MBS) located at $L_M = (x_M, y_M)$ and a known hotspot location, $L_H = (x_H, y_H)$, as indicated in Fig. 1. Hotspots locations can be calculated from users locations that can be obtained using UE localisation schemes such as observed time difference of arrival (OTDoA) [17] or self-reported GPS coordinates. Hotspots can also be predicted using historical records and deep learning as demonstrated in [18]. To improve the spectral efficiency and increase total system throughput, a dedicated DBS is deployed in the area of hotspot location [19]. The deployed DBS is backhaul-connected to the MBS through FSO links provided by a set of DRSs. The channels established by these links can adopt similar assumptions to those presented in [9]. We omit them here since this work focuses solely on avoiding obstacles¹. Therefore, successive hops should not have any obstacles blocking the FSO path between them. Fig. 1 shows the case where the link between the MBS and the DRS is blocked by a building, whereas the link between the DRS and hotspot is visible. Furthermore, we assume that the DRSs are equipped with solar panels that provide energy to the on-board batteries whenever the DRSs is in a sunny location. The energy consumption and regeneration models are introduced below.

B. Power Consumption Model

Following [14], for each DRS n , $(1, \dots, N)$, the aerodynamic energy consumed over observation time t_o , is described as $E_{UAV,n} = P_{hov,n} \cdot t_o$ where $P_{hov,n}$ is the power consumption for hovering determined as:

$$P_{hov,n} = \sqrt{\frac{(m_n g)^3}{2\pi r_{p,n}^2 l_{p,n} \rho}}, \quad (1)$$

¹Optimizing transmission parameters for reliability and throughput is left for future work.

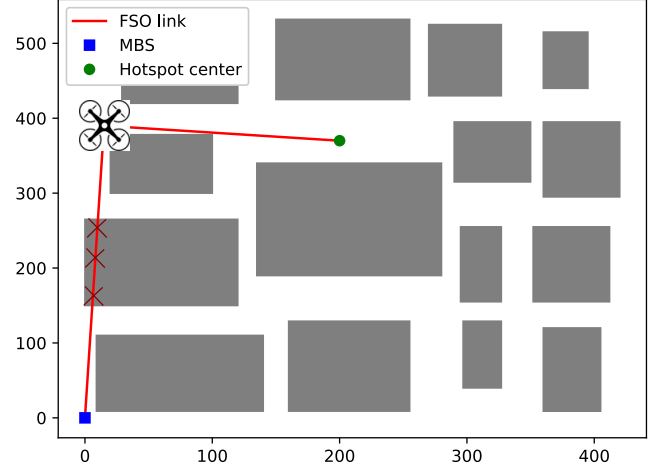


Figure 1. High-rise buildings with MBS and hotspot destination.

where m_n is the mass of the drone (in kg), and g denotes earth gravity (in $\frac{m}{s^2}$). The expression $2\pi r_{p,n}^2 l_{p,n}$ describes the total area of the UAV's propellers (in m^2), where $l_{p,n}$ is their number and $r_{p,n}$ is the radius of a single propeller, given in meters, and ρ determines the air density (in $\frac{kg}{m^3}$).

Next, the energy consumed to sustain an FSO link is described by $E_{back,n}(t_o) = P_{back,n} \cdot t_o$, where $E_{back,n}$ denotes the energy quantity in Wh spent to sustain the FSO backhaul link, through which the DRS relays the data to other nodes (including the MBS). $P_{back,n}$ defines the power required for the FSO link and is assumed to be constant.

C. Energy Harvesting Model

To evaluate the performance of the photovoltaic (PV) panels supporting drones, the following energy acquisition model is applied: $E_{PV,n}(t_o) = P_{PV,n} \cdot t_o$, where $P_{PV,n}$ describes the power generated by a single solar panel mounted on the n -th DRS's top cover. Assuming that the inclination angle of the solar collector's surface is equal to 0° , then as in [20]

$$P_{PV,n} = T_{atm} \cdot I_0 \cdot \delta \cdot \eta_{PV,n} \cdot S_{PV,n} \cdot \sin(\alpha), \quad (2)$$

where α is the solar altitude angle given in degrees, and $\eta_{PV,n}$ and $S_{PV,n}$ are the PV panel's efficiency factor and surface in square meters, respectively. Next, $T_{atm} I_0$ is the power of solar irradiation per unit area, where I_0 denotes the mean solar irradiation outside the atmosphere, both specified in W/m^2 , and T_{atm} specifies the atmospheric transmittance. Finally, to consider the impact of clouds on the acquired solar irradiation (and therefore on the amount of produced energy), the scaling parameter δ is used, which is a pseudorandom number generated from a uniform distribution between 0.8 and 1 that reduces the harvested solar energy.

D. Energy Storage System

Assuming perfect charging efficiency, the energy storage in observation time $t_o = t_s - t_{s-1}$ is formulated as [21] as:

$$E_{batt,n}(t_s) = E_{batt,n}(t_{s-1}) + E_{PV,n}(t_o) - E_{UAV,n}(t_o) - E_{back,n}(t_o), \quad (3)$$

where $E_{\text{batt},n}(t_s)$ is the energy accumulated inside the battery of the n -th drone at (t_s) time stamp.

III. FSO BACKHAUL SHORTEST PATH

A. Problem Formulation

Let the hotspot location be given by $L_H = (x_H, y_H)$, and the start location relating to the MBS as $L_M = (x_M, y_M)$. Then, the goal is to find a communication path from L_M to L_H that does not pass through any obstacle from the set of buildings shown in Fig. 1. Considering that the shortest path between obstacles is a set of straight lines that connects the source to destination via a possibly empty sequence of vertices of obstacles [22], our goal can be formulated as a visibility graph problem. In this case, an input graph G describes the set of geometric basic objects (e.g., convex polygons defined as the set of vertices and edges connecting them) and the resulting solution of the problem is a visibility graph G_v which contains all possible edges between any two vertices in G such that these two vertices are said to be *unobstructed* by any obstacle (i.e., having an obstacle-free LOS path between them). Then, the final solution can be obtained by applying a shortest path algorithm (e.g. Dijkstra's) to resulting graph to select the locations in which DRSs should be deployed to serve as backhaul nodes. In this paper we utilize Lee's algorithm presented in [16], taking advantage from its simplicity.

B. Proposed DRS Placement Algorithm

Given a map of the obstacles, we extract the graph $G(V, E)$ containing all the vertices V and edges E that define the buildings (i.e. building corners and building edges in the top view, respectively). We add to the set of vertices, V , the two points defining the start and end locations given by L_M and L_H , respectively, so that their visibility tree is also computed. Then we implement Lee's algorithm for each $v_i \in V$ to obtain the complete visibility graph G_v as follows [23]:

- 1) Initialize a horizontal scan line, \vec{s} , starting from the center vertex $c = v_i$ and pointing rightwards.
- 2) Sort all other vertices $\{v_j \in V - v_i\}$ in ascending order according to the angle θ_j between \vec{s} and \vec{cv}_j (i.e. by rotating \vec{s} counter-clockwise) inside a data structure A .
- 3) In another data structure, E_s , sort all the edges that are intersecting with \vec{s} in ascending order according to their distance from c , along with the distance magnitude. Clearly, the first edge is the only one that c can see.
- 4) Rotate \vec{s} to every vertex v_j in order of θ_j in A ; at every vertex, check any edge that v_j is a part of, and either add or remove this edge from E_s appropriately if \vec{s} would intersect this edge or not at the next rotation step.
- 5) At every rotation step check if the distance to v_j is less than the distance to the closest edge in E_s ; if so, then v_j is visible and it is added to the visibility tree of v_i , otherwise not.

After obtaining $G_v(V_g, E_g)$, each edge $E_k = \{v_i, v_j\}$ is assigned a cost given by

$$D = \frac{d(v_i, v_j)}{d_{\max}} + 1, \quad (4)$$

whereas $d(v_i, v_j)$ is the Euclidean distance between the two endpoints, and d_{\max} is a normalizing factor which limits the distance cost to $[0, 1]$ and can be set to the maximum distance between any two points in the considered area. The reason for defining the cost in such a way is that we want to obtain the shortest path in terms of hops primarily and then considering the link distance as a secondary objective. The additional value of 1 causes that choosing an edge increases the number of hops and therefore the number of DRSs. Finally, we can apply Dijkstra's algorithm on G_v with edges costs defined as in (4) to find the shortest communications path.

IV. PROPOSED SOLAR POWERED DRS PLACEMENT

To improve energy efficiency, in this paper we consider solar-powered DRSs and target the problem of their placement in a sunny environment with shadows resulting from buildings. The goal is to leverage the previously introduced energy generation system in order to prolong the deployment duration of DRSs and reduce the number of trips required by each DRS to return to its deployment base in order to recharge its battery.

A. Sunny Points Search

Since the DRSs should be placed in sunny locations, the first step is to find the set of possible points at a given hour in a day that are sunny (i.e., not shadowed by any building). A good starting point which guides us towards finding the shortest path is the set of building vertices V which we used in the previous section. Thus, given the sun altitude and azimuth angles, α and ϕ , and the set of obstacles defined by $G(V, E)$, we are able to test any point of interest if it falls within any shadow caused by a building in the direction $-\phi$ with a length of $\frac{h_B - h_{UAV}}{\tan(\alpha)}$ such that h_B and h_{UAV} define the heights of the building and the UAV, respectively. To find the set of sunny points V_s we perform the following steps for every vertex $v_i = (x_i, y_i) \in V$. Let $v'_i = (x'_i, y'_i)$ be the point in the interior of the polygon of which v_i is a vertex such that v'_i is equidistant from the two edges connected to v_i with a distance of D_T (see Fig. 2). First, we create a grid of test points around v_i denoted as $V_T = \{(x_j, y_j) \mid x_j = x'_i \pm nD_T, y_j = y'_i \pm nD_T, \text{ and } n = 1, 2, \dots, C_T, \text{ and } (x_j, y_j) \notin \{(x'_i, y'_i), (x'_i, y_i), (x_i, y'_i), (x_i, y_i)\}\}$ whereas we perform subtraction along the x-axis when $x_T < x'_i$, otherwise addition. Likewise along the y-axis. C_T and D_T determine the number of test points and the spacing between them, respectively. An example is shown in Fig. 2. The initial point is invalid because it's within the building, and we discard the points that are on the edges to consider irregularities in the building surface that could obstruct the light (e.g. balconies, advertisements, etc.). These points are then sequentially tested starting with the points closest to the building such that if and when a point is found to be in a sunny spot, then this point is added to V_s and the search stops.

B. DRS Placement in Sunny Spots Algorithm

Having obtained the set V_s of sunny locations, we can now apply Lee's algorithm (see Subsection III-B) however this time

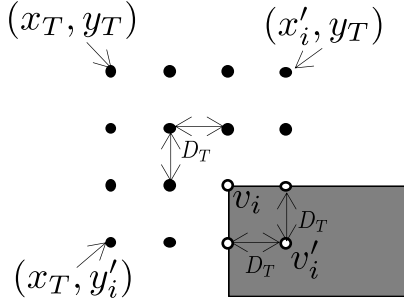


Figure 2. Test points grid for finding sunny spots for $C_T = 4$.

Table I. Simulation Parameters

Parameter	Value
Longitude	3.70427144 °W
Latitude	40.41872533 °N
UAV hovering height (h_{UAV})	20 m
Mean solar irradiation outside the atmosphere (I_0)	1353 W/m ² [20]
Efficiency of used solar cell type (η_{PV})	0.2
Area covered by the solar panels (S_{PV})	1 m ² [15]
UAV's mass (m)	4 kg [15]
Radius of UAV's single propeller (r_p)	0.25 m
Number of UAV's propellers (l_p)	4
UAV's battery capacity	222 Wh [15]
FSO backhaul link's power consumption (P_{back})	200 mW [8]
Distance cost normalizing factor (d_{max})	700 m
Width of test points (C_T)	5
Spacing between test points (D_T)	7 m

with the set of vertices (and points) being defined as $V' = \{V \cup V_s \cup \{L_H, L_M\}\}$. This will also result in obtaining the visibility trees for the new points of V_s . After obtaining the visibility graph, we again perform Dijkstra's algorithm with the cost function defined for every edge $E_k = \{v_i, v_j\}$ as follows

$$D = \begin{cases} \frac{d(v_i, v_j)}{d_{max}} + 1, & \text{if } v_j \in V_s, \\ \frac{d(v_i, v_j)}{d_{max}} + 100 & \text{otherwise.} \end{cases} \quad (5)$$

The cost function defined in (5) aims to penalize selecting a shadowed spot by increasing the hop penalty to 100. This results in avoiding any shadowed spots whenever possible.

V. SIMULATION AND RESULTS

In simulations we considered a location in Madrid, Spain, for the solar calculations during the whole day period of 24 hours. We assumed the environment model shown in Fig. 1 where a backhaul is provided to the drone serving users at the hotspot L_H . The simulation parameters are listed in Table I.

A. Placement of DRSs

Figure 3 shows the placement locations of DRSs along with the shadowed areas for 6 different timings during the day, including the whole night period with no sun. The algorithm is able to find a path of sunny locations at all time instants without selecting any shadowed hop as can be seen. An interesting observation is that the number of hops or required number of DRSs is reduced to two with a total traversed distance of 617 m between 7 am and 7 pm compared with

three required hops during the night and a total distance of 490 m. This indicates that the criteria of finding the shortest path using obstacles vertices might not be the best choice whereas such policy does not always yield the least hops path, however, it does indeed result in the shortest path. A different point selection mechanism which would focus on reducing the number of hops and increasing the efficiency of the search relatively to the mechanism introduced in this work can be the target of future work with the help pre-calculated sun maps.

B. Sustainability

We can observe the number of new DRS arrivals from deployment center per hour in Figure 4a, and the number of DRS return flights per hour in Figure 4b. Arrivals and returns can occur two cases. Either to recharge, or because a new DRS is needed or became redundant (notice the extra arrival at 18 in Figure 4a because a new drone is needed as shown in Figure 3e). Both figures plot the results with and without RESs. Clearly both counts are greatly reduced during the hours where the sun elevation angle is above zero in the case where solar panels are employed. In total, over the duration of 24 hours, 115 trips of DRSs are required to provide a backhaul to the hotspot location if RESs are not employed. In the case when RESs are used, around 74 trips are needed. That is 35% less required amount of battery recharges which amounts to $(\frac{115}{2} - \frac{75}{2})222Wh = 4440Wh$. Also, depending on the distance to the deployment center, the reduction in energy required for flying back can be substantial in scenarios where the DRSs have to travel a considerable distance.

VI. CONCLUSIONS

We have considered obstacles in the placement of DRSs utilizing FSO links and solar panels which was not targeted before in literature to our best knowledge. In this context, we presented how visibility graphs and shortest path algorithms can be leveraged to solve this type of problems. Furthermore, for a given scenario, we showed the gain in utilizing solar panels in terms of required number of recharge trips.

REFERENCES

- [1] J. G. Andrews, S. Buzzi, W. Choi, S. V. Hanly, A. Lozano, A. C. K. Soong, and J. C. Zhang, "What will 5G be?," *IEEE Journal on Selected Areas in Communications*, vol. 32, no. 6, pp. 1065–1082, 2014.
- [2] S. Hayat, E. Yanmaz, and R. Muzaffar, "Survey on unmanned aerial vehicle networks for civil applications: A communications viewpoint," *IEEE Comm. Surveys Tutorials*, vol. 18, no. 4, pp. 2624–2661, 2016.
- [3] A. Fotouhi, H. Qiang, M. Ding, M. Hassan, L. G. Giordano, A. Garcia-Rodriguez, and J. Yuan, "Survey on UAV cellular communications: Practical aspects, standardization advancements, regulation, and security challenges," *IEEE Communications Surveys Tutorials*, vol. 21, no. 4, pp. 3417–3442, 2019.
- [4] U. Siddique, H. Tabassum, E. Hossain, and D. I. Kim, "Wireless backhauling of 5G small cells: challenges and solution approaches," *IEEE Wireless Communications*, vol. 22, no. 5, pp. 22–31, 2015.
- [5] A. U. Chaudhry and H. Yanikomeroglu, "Free space optics for next-generation satellite networks," *IEEE Consumer Electronics Magazine*, vol. 10, no. 6, pp. 21–31, 2021.
- [6] M. Najafi, H. Ajam, V. Jamali, P. D. Diamantoulakis, G. K. Karagiannis, and R. Schober, "Statistical modeling of the FSO fronthaul channel for UAV-based communications," *IEEE Transactions on Communications*, vol. 68, no. 6, pp. 3720–3736, 2020.

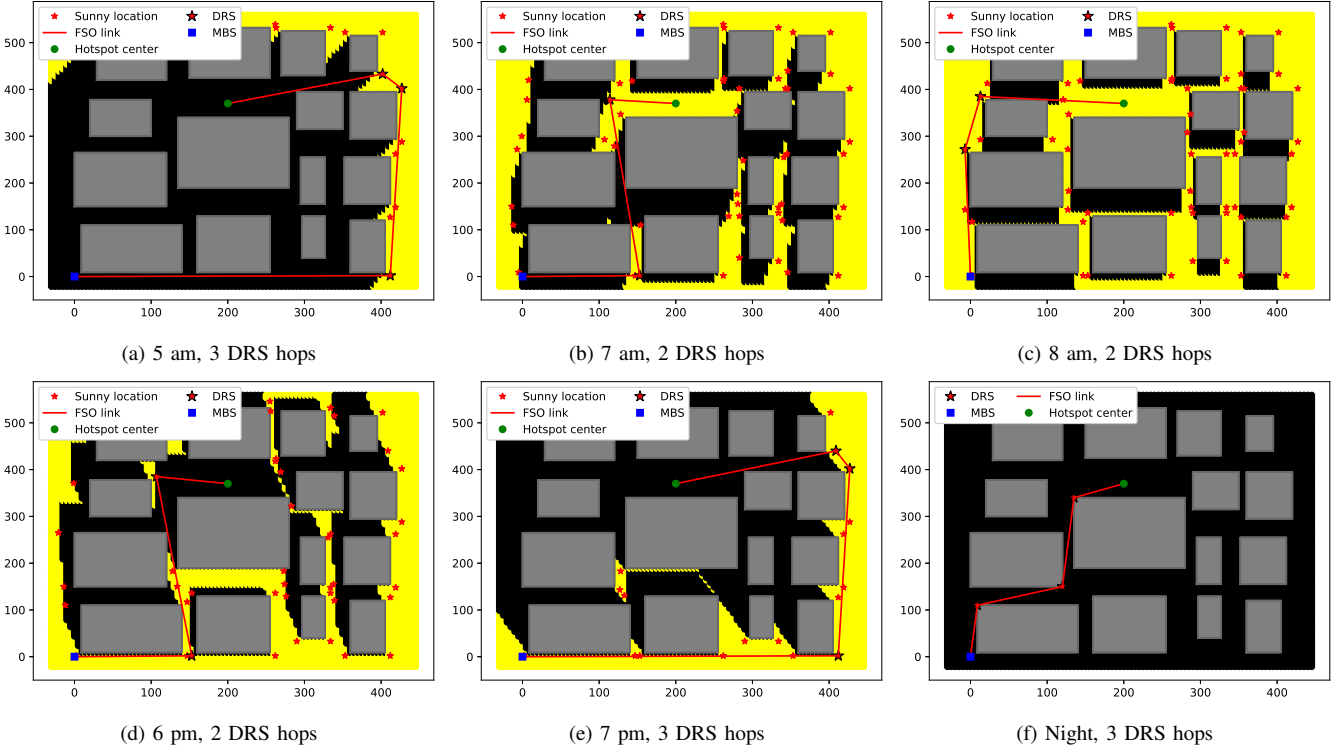


Figure 3. DRSs placements at different hours of the day.

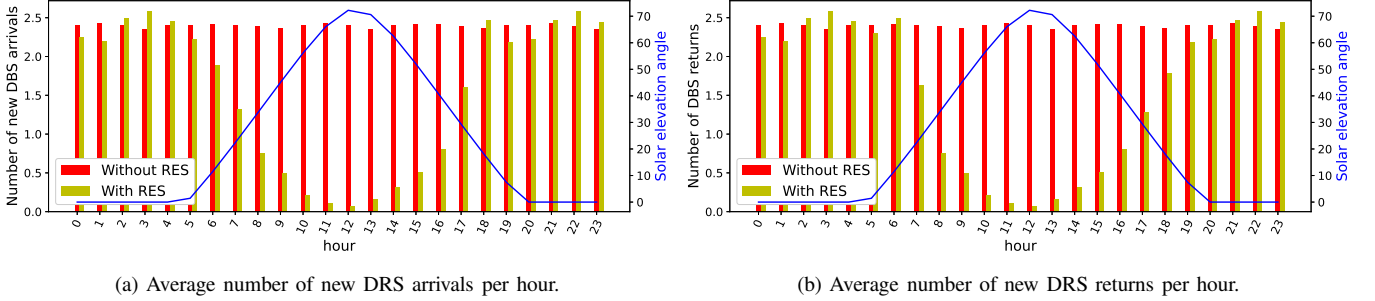


Figure 4. Required number of DRS trips back and forth to the charging location.

- [7] A. Kaadan, H. H. Refai, and P. G. LoPresti, "Multielement FSO transceivers alignment for inter-uav communications," *Journal of Light-wave Technology*, vol. 32, no. 24, pp. 4785–4795, 2014.
- [8] M. Alzenad, M. Z. Shakir, H. Yanikomeroglu, and M.-S. Alouini, "FSO-based vertical backhaul/fronthaul framework for 5G+ wireless networks," *IEEE Communications Magazine*, vol. 56, no. 1, pp. 218–224, 2018.
- [9] H. Ajam, M. Najafi, V. Jamali, and R. Schober, "Ergodic sum rate analysis of UAV-based relay networks with mixed RF-FSO channels," *IEEE Open Journal of the Communications Society*, vol. 1, pp. 164–178, 2020.
- [10] W. Fawaz, C. Abou-Rjeily, and C. Assi, "UAV-aided cooperation for FSO communication systems," *IEEE Communications Magazine*, vol. 56, no. 1, pp. 70–75, 2018.
- [11] A. Al-Hourani, "Interference modeling in low-altitude unmanned aerial vehicles," *IEEE Wireless Communications Letters*, vol. 9, no. 11, pp. 1952–1955, 2020.
- [12] Y. Zeng and R. Zhang, "Energy-efficient uav communication with trajectory optimization," *IEEE Transactions on Wireless Communications*, vol. 16, no. 6, pp. 3747–3760, 2017.
- [13] S. Morton, R. D'Sa, and N. Papanikolopoulos, "Solar powered UAV: Design and experiments," in *2015 IEEE/RSJ International Conference on Intelligent Robots and Systems (IROS)*, pp. 2460–2466, 2015.
- [14] S. Sekander, H. Tabassum, and E. Hossain, "Statistical performance modeling of solar and wind-powered UAV communications," *IEEE Transactions on Mobile Computing*, vol. 20, no. 8, pp. 2686–2700, 2021.
- [15] Y. Sun, D. Xu, D. W. K. Ng, L. Dai, and R. Schober, "Optimal 3D-trajectory design and resource allocation for solar-powered UAV communication systems," *IEEE Transactions on Communications*, vol. 67, no. 6, pp. 4281–4298, 2019.
- [16] D. Lee, *Proximity and Reachability in the Plane*. University of Illinois at Urbana-Champaign, 1978.
- [17] J. A. del Peral-Rosado, J. M. Parro-Jiménez, J. A. López-Salcedo, G. Seco-Granados, P. Crosta, F. Zanier, and M. Crisci, "Comparative results analysis on positioning with real LTE signals and low-cost hardware platforms," in *2014 7th ESA Workshop on Satellite Navigation Technologies and European Workshop on GNSS Signals and Signal Processing (NAVITEC)*, pp. 1–8, 2014.
- [18] Y. Liu, X. Wang, G. Boudreau, A. B. Sediq, and H. Abou-zeid, "Deep learning based hotspot prediction and beam management for adaptive virtual small cell in 5G networks," *IEEE Transactions on Emerging Topics in Computational Intelligence*, vol. 4, no. 1, pp. 83–94, 2020.
- [19] B. Galkin, J. Kibilda, and L. A. DaSilva, "Deployment of UAV-mounted access points according to spatial user locations in two-tier cellular networks," in *2016 Wireless Days (WD)*, pp. 1–6, 2016.
- [20] S. Dimitriou, S. Kapsalis, P. Panagiotou, and K. Yakinthos, "Energy efficiency improvement potential of a tactical BWB UAV using renewable energy sources," in *2020 International Conference on Unmanned Aircraft Systems (ICUAS)*, pp. 1384–1391, 2020.

- [21] A. Jahid, M. K. H. Monju, M. E. Hossain, and M. F. Hossain, "Renewable energy assisted cost aware sustainable off-grid base stations with energy cooperation," *IEEE Access*, vol. 6, pp. 60900–60920, 2018.
- [22] T. Lozano-Pérez and M. A. Wesley, "An algorithm for planning collision-free paths among polyhedral obstacles," *Commun. ACM*, vol. 22, p. 560–570, oct 1979.
- [23] D. Coleman, "Lee's $O(n^2 \log n)$ visibility graph algorithm implementation and analysis," 2012.